

Control of a Filter Cavity with Coherent Control Sidebands

Naoki Aritomi,^{1,2,*} Matteo Leonardi,² Eleonora Capocasa,² Yuhang Zhao,^{2,3} and Raffaele Flaminio^{4,2}

¹*Department of Physics, University of Tokyo, 7-3-1 Hongo, Tokyo, 113-0033, Japan*

²*National Astronomical Observatory of Japan, 2-21-2 Osawa, Mitaka, Tokyo, 181-8588, Japan*

³*Department of Astronomical Science, SOKENDAI, 2-21-2 Osawa, Mitaka, Tokyo, 181-8588, Japan*

⁴*Laboratoire d'Annecy-le-Vieux de Physique des Particules (LAPP),
Universit Savoie Mont Blanc, CNRS/IN2P3, F-74941 Annecy-le-Vieux, France*

(Dated: March 3, 2022)

For broadband quantum noise reduction of gravitational-wave detectors, frequency-dependent squeezed vacuum states realized using a filter cavity is a mature technique and will be implemented in Advanced LIGO and Advanced Virgo from the fourth observation run. To obtain the benefit of frequency-dependent squeezing, detuning and alignment of the filter cavity with respect to squeezed vacuum states must be controlled accurately. To this purpose we suggest a new length and alignment control scheme, using coherent control sidebands which are already used to control the squeezing angle. Since both squeezed vacuum states and coherent control sidebands have the same mode matching conditions and almost the same frequency, detuning and alignment of the filter cavity can be controlled accurately with this scheme. In this paper, we show the principle of this scheme and its application to a gravitational-wave detector.

I. INTRODUCTION

Gravitational-waves (GW) were first detected by Advanced LIGO in 2015 [1] and since then many more GW observations were performed by Advanced LIGO and Advanced Virgo [2]. To increase the number of detections, the sensitivity of the detectors must be constantly improved. One of the main noise sources which limits the sensitivity of GW detectors is the so-called quantum noise. Quantum noise is divided into shot noise, which limits the sensitivity at high frequency and radiation pressure noise, which limits the sensitivity at low frequency. An effective way to reduce quantum noise is to inject squeezed vacuum states into the interferometer [3]. The reduction of quantum noise with squeezing was realized for the first time at GEO600 [4] and it has been recently implemented also in Advanced LIGO and Advanced Virgo since the beginning of the third observation run (O3) [5, 6]. However, conventional frequency-independent phase squeezed vacuum states increases radiation pressure noise at low frequency while it reduces shot noise at high frequency. For broadband quantum noise reduction, frequency-dependent squeezing produced with a filter cavity is the most promising technique [7]. Advanced LIGO and Advanced Virgo plan to implement frequency-dependent squeezing with 300 m filter cavities from the fourth observation run (O4) [8]. In order to achieve the frequency-dependence below 100 Hz, the cavity has to be operated in a detuned configuration and it needs a storage time of about 3 ms.

Demonstration of frequency-dependent squeezing below 100 Hz, necessary for broadband quantum noise reduction in GW detectors, has been recently achieved with a 300 m filter cavity [9].

One of main challenges in the production of frequency-dependent squeezing by using filter cavities is the length and alignment control of the filter cavity itself. In fact, since squeezing is a vacuum state with no coherent amplitude, it is not suitable to provide the error signals necessary for the control. The use of auxiliary fields is therefore needed. In previous experiments [9], the filter cavity was controlled with an auxiliary green field with a wavelength of 532 nm while the squeezed field is at the GW detector laser wavelength, 1064 nm. However, controlling length and alignment of the filter cavity with the green field does not ensure the alignment of squeezed field to the filter cavity, since the overlap of the green and squeezed field can drift. In addition, fluctuation of the relative phase delay between green and infrared induced by anisotropies or temperature dependency of the cavity mirror coating can lead to a detuning fluctuation [10]. The squeezed field is produced by a parametric down-conversion process inside an optical parametric oscillator (OPO). The use of an auxiliary field which is resonating inside the OPO, ensures that it is perfectly spatially overlapped with the squeezed field. For what concern the length control of the filter cavity, a recent work has successfully tested a scheme which uses an additional auxiliary field with a small frequency offset with respect to the squeezing field injected into the OPO [11].

In this paper, we suggest a new length and alignment control scheme whose error signal is provided by the so-called coherent control field. Such field is included in all the squeezed vacuum sources for GW detectors and it is used to control the squeezing angle [12]. Since the coherent control sidebands (CCSB) are produced inside the OPO together with the squeezed vacuum states, they have the same mode matching conditions and almost the same frequency. The relative frequency of carrier and CCSB can be controlled accurately with a frequency offset phase locked loop and can be tuned so that carrier is properly detuned. Such difference is only of few

* aritomi@granite.phys.s.u-tokyo.ac.jp

MHz which makes negligible any possible effect due to the coating. Therefore, length and alignment control with CCSB ensures proper detuning and alignment of the squeezed vacuum states to the filter cavity.

This paper is organized as follows: in section II A and II B, the error signal for the length and alignment control of the filter cavity are theoretically derived. In section II C, the application of such control scheme to a GW detector is presented. In section II D, the coupling between the coherent control loop and the filter cavity length control loop is studied. In section II E, reshaping of frequency-dependent phase noise and an updated squeezing degradation budget with this control scheme are presented. In section III, the computation of noise requirements to ensure the feasibility of such technique is presented.

II. PRINCIPLE

A. Filter cavity error signal

When coherent control field, which is detuned by Ω_{cc} with respect to carrier frequency ω_0 , is injected into OPO, a sideband which is detuned by $-\Omega_{cc}$ is generated by nonlinear effect [12]. Coherent control field passing through OPO can be written as

$$E_{cc} = \frac{1}{2} \left(a_{cc} \frac{g+1}{\sqrt{g}} \right) e^{i(\omega_0 + \Omega_{cc})t} + \frac{1}{2} \left(a_{cc} \frac{g-1}{\sqrt{g}} \right) e^{i(\omega_0 - \Omega_{cc})t + i2\phi_{green}} \quad (1)$$

where a_{cc} is the amplitude of the coherent control field, g is the nonlinear gain, ϕ_{green} is the relative phase of the coherent control field and its sideband generated by OPO. ϕ_{green} is kept constant by the coherent control loop to control the squeezing angle. There are two coherent control loops and ϕ_{green} is controlled by the first coherent control loop. We assume that ϕ_{green} is kept 0, but has residual noise around 0, $\phi_{green} = \delta\phi_{green} \ll 1$.

To obtain proper frequency-dependent squeezing from a filter cavity, the carrier must be detuned properly from the resonance of the filter cavity. By choosing the frequency of coherent control field (Ω_{cc}) as follows, the coherent control field can be resonant inside the filter cavity while the carrier is properly detuned (FIG. 1):

$$\Omega_{cc} = n \times \omega_{FSR} + \Delta\omega_{fc,0} \quad (2)$$

where n is an integer number, $\omega_{FSR} = 2\pi f_{FSR}$ is the free spectral range of the filter cavity and $\Delta\omega_{fc,0}$ is the optimal filter cavity detuning with respect to carrier. In this condition, the coherent control sideband at $-\Omega_{cc}$ is detuned by $-2\Delta\omega_{fc,0}$ with respect to the filter cavity resonance and so almost reflected by the filter cavity.

The coherent control sidebands reflected by the filter cavity is

$$E_{cc} = a_+ r_+ e^{i(\omega_0 + \Omega_{cc})t} + a_- r_- e^{i(\omega_0 - \Omega_{cc})t + i2\delta\phi_{green}} \quad (3)$$

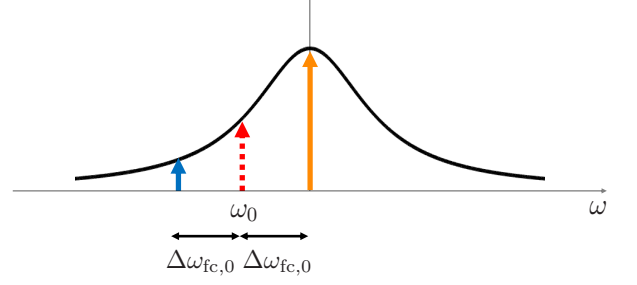


FIG. 1. Frequency relationship inside the filter cavity. Red dashed line is carrier, orange and blue lines are coherent control sidebands.

where a_{\pm} is

$$a_{\pm} = a_{cc} \frac{g \pm 1}{2\sqrt{g}} \quad (4)$$

and $r_{\pm} = r_{fc}(\pm\Delta\omega_{fc,0}, \Delta\omega_{fc})$ is the complex reflectivity of the filter cavity and can be written as [13]

$$r_{fc}(\pm\Delta\omega_{fc,0}, \Delta\omega_{fc}) \simeq 1 - \frac{2 - \epsilon}{1 + i\xi(\pm\Delta\omega_{fc,0}, \Delta\omega_{fc})} \quad (5)$$

where

$$\epsilon = \frac{f_{FSR}}{\gamma_{fc}} \Lambda_{rt}^2 \quad (6)$$

$$\xi(\pm\Delta\omega_{fc,0}, \Delta\omega_{fc}) = \frac{\pm\Delta\omega_{fc,0} - \Delta\omega_{fc}}{\gamma_{fc}} \quad (7)$$

with γ_{fc} the filter cavity half-bandwidth and Λ_{rt} the filter cavity round trip losses. $\Delta\omega_{fc}$ is a variable which represents the filter cavity detuning.

Amplitude and phase of the filter cavity reflectivity for CCSB can be written as

$$\begin{aligned} \rho_{\pm}(\Delta\omega_{fc}) &= |r_{fc}(\pm\Delta\omega_{fc,0}, \Delta\omega_{fc})| \\ &= \sqrt{1 - \frac{(2 - \epsilon)\epsilon}{1 + \xi^2(\pm\Delta\omega_{fc,0}, \Delta\omega_{fc})}} \end{aligned} \quad (8)$$

$$\begin{aligned} \alpha_{\pm}(\Delta\omega_{fc}) &= \arg(r_{fc}(\pm\Delta\omega_{fc,0}, \Delta\omega_{fc})) \\ &= \arg(-1 + \epsilon + \xi^2(\pm\Delta\omega_{fc,0}, \Delta\omega_{fc})) \\ &\quad + i(2 - \epsilon)\xi(\pm\Delta\omega_{fc,0}, \Delta\omega_{fc}) \end{aligned} \quad (9)$$

Filter cavity error signal can be obtained by detecting the beat note of the CCSB:

$$\begin{aligned} P_{cc} &= \left| a_+ r_+ e^{i(\omega_0 + \Omega_{cc})t} + a_- r_- e^{i(\omega_0 - \Omega_{cc})t + i2\delta\phi_{green}} \right|^2 \\ &= (\text{DC term}) + 2a_+ a_- \text{Re}\{r_+ r_-^* e^{i(2\Omega_{cc}t - 2\delta\phi_{green})}\} \end{aligned} \quad (10)$$

Demodulating this signal by $\sin(2\Omega_{cc}t - \alpha_-(\Delta\omega_{fc,0}))$ (In-phase) and $\cos(2\Omega_{cc}t - \alpha_-(\Delta\omega_{fc,0}))$ (Quadrature)

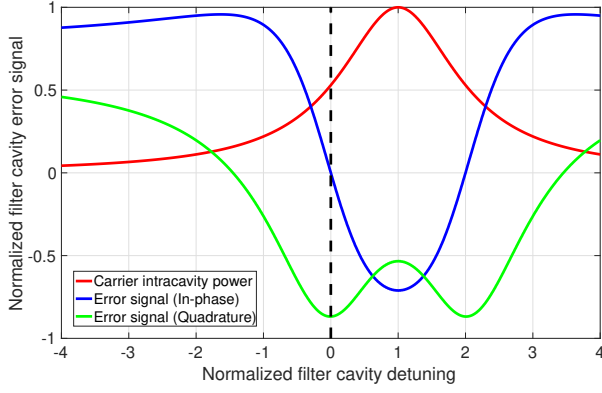


FIG. 2. Filter cavity error signal normalized with respect to a_+a_- . The horizontal axis is the filter cavity detuning normalized with respect to $\Delta\omega_{fc,0}$. Red line is intracavity power of carrier in the filter cavity, blue and green lines are the filter cavity error signal (In-phase and Quadrature). The filter cavity error signal (In-phase) becomes 0 when $\Delta\omega_{fc} = \Delta\omega_{fc,0}$.

and low-passing it, filter cavity error signal as a function of the filter cavity detuning $\Delta\omega_{fc}$ is

$$P_I = -a_+a_- \rho_+(\Delta\omega_{fc}) \rho_-(\Delta\omega_{fc}) \times \sin(\alpha_+(\Delta\omega_{fc}) - \alpha_-(\Delta\omega_{fc}) + \alpha_-(\Delta\omega_{fc,0}) - 2\delta\phi_{\text{green}}) \quad (11)$$

$$P_Q = a_+a_- \rho_+(\Delta\omega_{fc}) \rho_-(\Delta\omega_{fc}) \times \cos(\alpha_+(\Delta\omega_{fc}) - \alpha_-(\Delta\omega_{fc}) + \alpha_-(\Delta\omega_{fc,0}) - 2\delta\phi_{\text{green}}) \quad (12)$$

The relative phase noise of CCSB $\delta\phi_{\text{green}}$ is a noise source for the filter cavity error signal. When $\delta\phi_{\text{green}} = 0$, the filter cavity error signal (11), (12) normalized with respect to a_+a_- is shown in FIG. 2. The parameters used in this calculation are shown in TABLE I.

Filter cavity length noise δL_{fc} causes detuning noise $\delta\Delta\omega_{fc}$ as follows,

$$\delta\Delta\omega_{fc} = \frac{\omega_0}{L_{fc}} \delta L_{fc} \quad (13)$$

where L_{fc} is filter cavity length. When $\Delta\omega_{fc} = \Delta\omega_{fc,0} + \delta\Delta\omega_{fc}$, the filter cavity error signal (In-phase) (11) is

$$\begin{aligned} P_I &\propto -\sin(\alpha_+(\Delta\omega_{fc,0} + \delta\Delta\omega_{fc}) - \alpha_-(\Delta\omega_{fc,0} + \delta\Delta\omega_{fc}) + \alpha_-(\Delta\omega_{fc,0})) \\ &\simeq -\sin(\alpha_+(\Delta\omega_{fc,0} + \delta\Delta\omega_{fc})) \simeq 2 \frac{\delta\Delta\omega_{fc}}{\gamma_{fc}} = \frac{8\mathcal{F}}{\lambda} \delta L_{fc} \\ &= 9.7 \text{ mrad} \left(\frac{1064 \text{ nm}}{\lambda} \right) \left(\frac{\mathcal{F}}{4360} \right) \left(\frac{\delta L_{fc}}{0.3 \text{ pm}} \right) \end{aligned} \quad (14)$$

where λ is wavelength of carrier, \mathcal{F} is filter cavity finesse. Here we only considered the phase of coherent control field which is on resonance of the filter cavity since this phase noise is dominant compared with the phase noise of the other coherent control sideband which is off resonance of the filter cavity. We also assumed $\epsilon \ll 1$ and

TABLE I. Parameters for 300 m filter cavity [15].

Parameter	Symbol	Value
Filter cavity length	L_{fc}	300 m
Filter cavity half-bandwidth	γ_{fc}	$2\pi \times 57.3 \text{ Hz}$
Filter cavity detuning	$\Delta\omega_{fc,0}$	$2\pi \times 54 \text{ Hz}$
Filter cavity finesse	\mathcal{F}	4360
Filter cavity input mirror transmissivity	t_{in}^2	0.00136
Filter cavity round trip losses	Λ_{rt}^2	80 ppm
Injection losses	Λ_{inj}^2	5 %
Readout losses	Λ_{ro}^2	5 %
Mode-mismatch losses (squeezer-filter cavity)	Λ_{mmFC}^2	2 %
Mode-mismatch losses (squeezer-local oscillator)	Λ_{mmLO}^2	5 %
Frequency-independent phase noise (rms)	$\delta\phi$	30 mrad
Filter cavity length noise (rms)	δL_{fc}	0.3 pm
Injected squeezing	σ_{dB}	9 dB

$\delta\Delta\omega_{fc}/\gamma_{fc} \ll 1$, which is true for parameters shown in TABLE I. Since the relative phase noise of CCSB $\delta\phi_{\text{green}}$ can be stabilized by the first coherent control loop below 1.7 mrad [14], the filter cavity error signal (14) can be obtained with a good enough SNR.

B. Alignment of a filter cavity

Coherent control sidebands can be also used to control alignment of a filter cavity by wavefront sensing [16].

Misalignment of the filter cavity axis with respect to input beam axis γ and misalignment of immediately reflected beam axis with respect to the filter cavity axis γ_r can be written as

$$\gamma = \delta x/w_0 + i\delta\theta/\theta_0 \quad (15)$$

$$\gamma_r = \delta x'/w_0 + i\delta\theta'/\theta_0 \quad (16)$$

where w_0 is the beam radius at waist position, $\theta_0 = 2/kw_0$ is the beam divergence, k is the wave number. δx , $\delta x'$ represent the transverse displacement in x axis direction and $\delta\theta$, $\delta\theta'$ represent the tilt around y axis, where z axis is the beam axis and y axis is orthogonal to the x, z axis. $z = 0$ is the beam waist position.

We define C and S as

$$C = r_{c0}\gamma_r + r_{c1}\gamma^* \quad (17)$$

$$S = r_{s0}\gamma_r + r_{s1}\gamma^* \quad (18)$$

where r_{c0} , r_{c1} are the filter cavity reflectivity of Hermite-Gaussian (HG) 00 and 10 mode of coherent control field and r_{s0} , r_{s1} are the filter cavity reflectivity of HG 00 and 10 mode of coherent control sideband. $2\Omega_{cc}$ term of the filter cavity error signal (10) can be written as (see

Appendix A)

$$\begin{aligned}
P_{cc}(2\Omega_{cc}) &\propto \text{Re}\{r_c r_s^* e^{i2\Omega_{cc}t}\} \\
&= \text{Re}\{(U_{00}r_{c0} - U_{10}C)(U_{00}^*r_{s0}^* - U_{10}^*S^*)e^{i2\Omega_{cc}t}\} \\
&= \text{Re}\{(U_{00}U_{00}^*r_{c0}r_{s0}^* - U_{00}U_{10}^*r_{c0}S^* \\
&\quad - U_{00}^*U_{10}r_{s0}^*C + U_{10}U_{10}^*CS^*)e^{i2\Omega_{cc}t}\} \quad (19)
\end{aligned}$$

where U_{00}, U_{10} are normalized Hermite-Gaussian modes and can be written as [17],

$$\begin{aligned}
U_{00}(x, y, z) &= \sqrt{\frac{2}{\pi w^2(z)}} \exp[-i(kz - \eta(z)) \\
&\quad - (x^2 + y^2) \left(\frac{1}{w^2(z)} + \frac{ik}{2R(z)} \right)] \quad (20)
\end{aligned}$$

$$U_{10}(x, y, z) = \frac{1}{\sqrt{2}} H_1 \left(\frac{\sqrt{2}x}{w(z)} \right) \exp(i\eta(z)) U_{00} \quad (21)$$

where H_1 is the 1st order Hermite polynomial, $w(z)$ is the beam radius, $\eta(z)$ is the gouy phase, $R(z)$ is the beam radius of curvature and can be written as

$$w(z) = w_0 \sqrt{1 + z^2/z_0^2} \quad (22)$$

$$\eta(z) = \arctan(z/z_0) \quad (23)$$

$$R(z) = z(1 + z_0^2/z^2) \quad (24)$$

$$z_0 = kw_0^2/2 \quad (25)$$

The wavefront sensing (WFS) signal W is given by the sum of the second and third term of (19). Defining $U = U_{00}U_{10}^*$,

$$\begin{aligned}
W &\propto \text{Re}\{(-Ur_{c0}(r_{s0}^*\gamma_r^* + r_{s1}^*\gamma) \\
&\quad - U^*r_{s0}^*(r_{c0}\gamma_r + r_{c1}\gamma^*))e^{i2\Omega_{cc}t}\} \\
&= \text{Re}\{(-r_{c0}r_{s0}^*(U\gamma_r^* + U^*\gamma_r) \\
&\quad - r_{c0}r_{s1}^*U\gamma - r_{c1}r_{s0}^*U^*\gamma^*)e^{i2\Omega_{cc}t}\} \quad (26)
\end{aligned}$$

Differential signal of W in x axis direction with a quadrant photo diode is

$$W_{\text{diff}} = \int \int dxdy \{W(x > 0) - W(x < 0)\} \quad (27)$$

Since

$$\int \int dxdy \{U(x > 0) - U(x < 0)\} = \sqrt{\frac{2}{\pi}} e^{-i\eta(z)} \quad (28)$$

WFS signal is

$$\begin{aligned}
W_{\text{diff}} &\propto \sqrt{\frac{2}{\pi}} \text{Re}\{(-r_{c0}r_{s0}^*(e^{-i\eta}\gamma_r^* + e^{i\eta}\gamma_r) \\
&\quad - r_{c0}r_{s1}^*e^{-i\eta}\gamma - r_{c1}r_{s0}^*e^{i\eta}\gamma^*)e^{i2\Omega_{cc}t}\} \quad (29)
\end{aligned}$$

Demodulating by $\sin(2\Omega_{cc}t - \alpha_-(\Delta\omega_{fc,0}))$ (In-phase) and low-passing it, first term of (29), which is proportional to filter cavity error signal, will disappear.

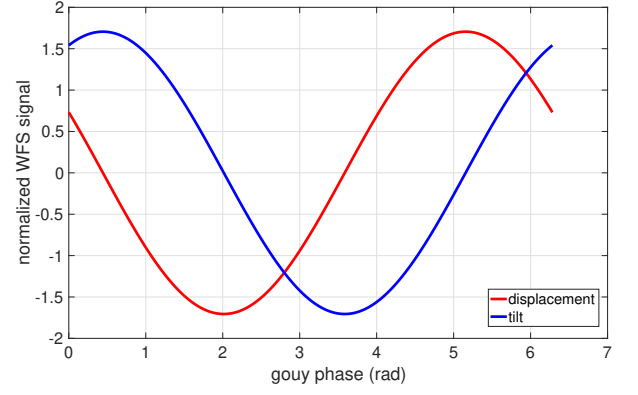


FIG. 3. Filter cavity WFS signal normalized with $-\sqrt{\frac{2}{\pi}}a_+a_-$. Red line is displacement signal with $\delta x = w_0$ and blue line is tilt signal with $\delta\theta = \theta_0$.

WFS signal after demodulation is

$$\begin{aligned}
W_I &= -\sqrt{\frac{2}{\pi}} a_+ a_- \\
&\times \{ \text{Re}(-r_{c0}r_{s1}^*e^{-i\eta}\gamma - r_{c1}r_{s0}^*e^{i\eta}\gamma^*) \sin \alpha_- (\Delta\omega_{fc,0}) \\
&\quad + \text{Im}(-r_{c0}r_{s1}^*e^{-i\eta}\gamma - r_{c1}r_{s0}^*e^{i\eta}\gamma^*) \cos \alpha_- (\Delta\omega_{fc,0}) \} \quad (30)
\end{aligned}$$

WFS signal is shown in FIG. 3. Displacement and tilt signal of the filter cavity can be obtained with two different gouy phase.

C. Experimental setup

An example of experimental setup when this scheme is implemented in GW detectors is shown in FIG. 4. Filter cavity error signal with CCSB can be obtained at output mode cleaner (OMC) reflection since CCSB are almost fully reflected by OMC while carrier almost transmits through OMC. The error signal is demodulated by $2\Omega_{cc}$ and fed back to the filter cavity length. The error signal of the first coherent control loop to control the relative phase between the green field injected into OPO and the coherent control field can be obtained at OPO reflection and fed back to the green field path length. The error signal of the second coherent control loop to control the relative phase between the carrier and the coherent control field is obtained at OMC transmission and fed back to phase locked loop (PLL) between interferometer laser and squeezer laser [18].

D. Coherent control error signal

The filter cavity control loop with CCSB affects the second coherent control loop which controls the relative phase between the coherent control field (CC) and the local oscillator (LO). In the case of GW detectors, the LO is

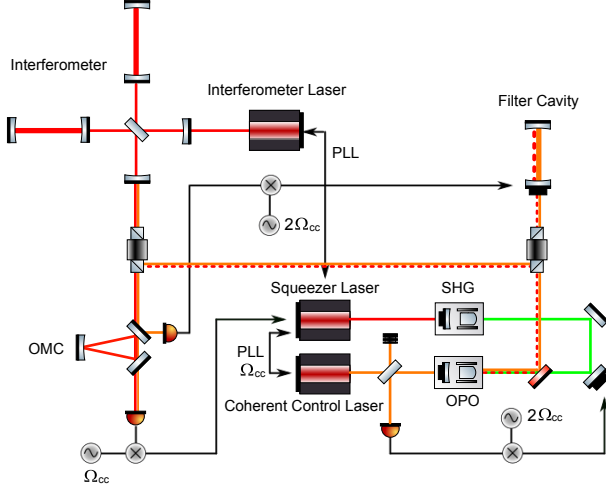


FIG. 4. An example of experimental setup. Red solid line is the carrier and red dashed line is the squeezed vacuum states. Orange line is the coherent control field. Green line is the green pump field which is produced by the second harmonic generator (SHG) and injected into the OPO.

the interferometer laser. In this section, we will calculate the error signal of the second coherent control loop. For simplicity, here we write $\rho_{\pm}(\Delta\omega_{fc}) = \rho_{\pm}$, $\alpha_{\pm}(\Delta\omega_{fc}) = \alpha_{\pm}$ and $\alpha_{\pm}(\Delta\omega_{fc,0}) = \alpha_{\pm,0}$.

Signal at OMC transmission is

$$\begin{aligned}
 P_{cc} &\propto \left| a_0 e^{i(\omega_0 t + \phi_{LO})} + a_+ \rho_+ e^{i(\omega_0 + \Omega_{cc})t + i(\phi_{CC} + \alpha_+)} \right. \\
 &\quad \left. + a_- \rho_- e^{i(\omega_0 - \Omega_{cc})t + i(\phi_{CC} + \alpha_- + 2\delta\phi_{green})} \right|^2 \\
 &= 2a_0 a_+ \rho_+ \cos(\Omega_{cc}t - \phi_{LO} + \phi_{CC} + \alpha_+) \\
 &\quad + 2a_0 a_- \rho_- \cos(\Omega_{cc}t + \phi_{LO} - \phi_{CC} - \alpha_- - 2\delta\phi_{green}) \\
 &\quad + (\text{DC term}) + (2\Omega_{cc} \text{ term})
 \end{aligned} \quad (31)$$

where a_0 is the relative amplitude of LO and ϕ_{LO}, ϕ_{CC} are the phase noise of LO and CC respectively.

Demodulating (31) by $\cos(\Omega_{cc}t + \theta_{dm})$ and low-passing it, where demodulation phase θ_{dm} is

$$\theta_{dm} = \frac{\alpha_{+,0} - \alpha_{-,0}}{2} \quad (32)$$

we find

$$\begin{aligned}
 P_1 &= a_0 a_+ \rho_+ \sin\left(-\phi_{LO} + \phi_{CC} + \alpha_{p,0} + \delta\alpha_+ + \frac{\pi}{2}\right) \\
 &\quad - a_0 a_- \rho_- \sin\left(\phi_{LO} - \phi_{CC} - \alpha_{p,0} - \delta\alpha_- - \frac{\pi}{2} - 2\delta\phi_{green}\right)
 \end{aligned} \quad (33)$$

where

$$\alpha_{p,0} = \frac{\alpha_{+,0} + \alpha_{-,0}}{2} \quad (34)$$

$$\delta\alpha_{\pm} = \alpha_{\pm} - \alpha_{\pm,0} \quad (35)$$

The squeezing angle ϕ_{sqz} is the relative phase between LO and CC reflected by the filter cavity and can be written as

$$\phi_{sqz} = \phi_{LO} - \phi_{CC} - \alpha_{p,0} \quad (36)$$

When the squeezing angle is different from $\pi/2$ (squeeze quadrature) by $\delta\phi_{sqz}$, (36) can be written as

$$\phi_{sqz} = \phi_{LO} - \phi_{CC} - \alpha_{p,0} = \frac{\pi}{2} + \delta\phi_{sqz} \quad (37)$$

The coherent control error signal (33) can be written as

$$\begin{aligned}
 P_1 &= a_0 a_+ \rho_+ \{ - (1 + a\rho) \delta\phi_{sqz} + 2(\delta\alpha_p(\Delta\omega_{fc}, a, \rho) \\
 &\quad + a\rho\delta\phi_{green}) \}
 \end{aligned} \quad (38)$$

where $a = a_-/a_+$ is the unbalance of amplitude of CCSB and $\rho = \rho_-/\rho_+$ is the unbalance of filter cavity reflectivity of CCSB. $\delta\alpha_p(\Delta\omega_{fc}, a, \rho)$ is

$$\delta\alpha_p(\Delta\omega_{fc}, a, \rho) = \frac{\delta\alpha_+ + a\rho\delta\alpha_-}{2} \quad (39)$$

The first term in (38) is the relative phase noise between CC and LO which does not include the phase noise coming from the filter cavity (frequency-independent phase noise), the second term is the phase noise of CCSB coming from the filter cavity length noise (frequency-dependent phase noise at the detuning frequency) and the third term is the phase noise coming from the relative phase noise of CCSB. The second term is the coupling from the filter cavity control loop which reshapes frequency-dependent phase noise as explained in the following section.

E. Reshaping of frequency-dependent phase noise

The coherent control error signal calculated in Sec. IID reshapes frequency-dependent phase noise which comes from the filter cavity length noise. This is caused by the coupling between the filter cavity length control loop and the coherent control loop as shown in FIG. 5.

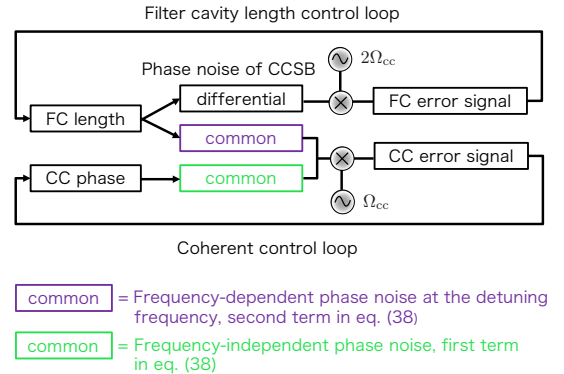


FIG. 5. Coupling between the filter cavity length control loop and the coherent control loop.

The fluctuation of the filter cavity length causes both differential and common phase noise of CCSB. The differential phase noise of CCSB is the filter cavity error signal while the common phase noise of CCSB is frequency-dependent phase noise at the detuning frequency, which is the second term in (38). This frequency-dependent phase noise at the detuning frequency couples to the coherent control loop and is suppressed by the feedback loop while the frequency-dependent phase noise is increased at high frequency. In this section, we will explain the detail calculation of the frequency-dependent phase noise with feedback of coherent control loop.

Calculation of frequency-dependent phase noise is described in [13] and the calculation of this section will use the same formalism. For more details of the computation, see Appendix B.

Assuming multiple incoherent noise parameters X_n in quantum noise \hat{N} have small Gaussian-distributed fluctuations with variance δX_n^2 , the average readout noise is given by

$$\hat{N}_{\text{avg}} \simeq \hat{N} + \sum_n \left(\frac{\hat{N}(X_n + \delta X_n) + \hat{N}(X_n - \delta X_n)}{2} - \hat{N} \right) \quad (40)$$

For frequency-independent phase noise, $X_n = \phi$ which is the injection squeezing angle. For the frequency-dependent phase noise, $X_n = \Delta\omega_{\text{fc},0}$ which is the filter cavity detuning.

First we will explain about the calculation of frequency-independent phase noise which is necessary in order to calculate frequency-dependent phase noise with feedback from coherent control loop. The transfer matrix of the squeezer can be written as a function of injection squeezing angle ϕ ,

$$\mathbf{S} = \mathbf{R}_\phi \begin{pmatrix} e^\sigma & 0 \\ 0 & e^{-\sigma} \end{pmatrix} \mathbf{R}_{-\phi} \quad (41)$$

where \mathbf{R} is a rotation matrix and $e^{-\sigma}$ is injection squeezing level. Frequency-independent phase noise can be represented by variations of injection squeezing angle, $\delta\phi$.

To calculate the effect of phase noise only, we restrict our discussion to an optimally matched filter cavity and no injection, readout losses. Noise due to vacuum fluctuations passing through the squeezer, \hat{N}_1 can be written as (see Appendix B)

$$\hat{N}_1(\phi) = A \cos^2 \phi + 2B \cos \phi \sin \phi + C \sin^2 \phi \quad (42)$$

$$A = (\rho_p^2 e^{-2\sigma} + \rho_m^2 e^{2\sigma})(\cos \alpha_p + \mathcal{K} \sin \alpha_p)^2 + (\rho_p^2 e^{2\sigma} + \rho_m^2 e^{-2\sigma})(\mathcal{K} \cos \alpha_p - \sin \alpha_p)^2 \quad (43)$$

$$B = (e^{2\sigma} - e^{-2\sigma})(\rho_m^2 - \rho_p^2) \times (\cos \alpha_p + \mathcal{K} \sin \alpha_p)(\mathcal{K} \cos \alpha_p - \sin \alpha_p) \quad (44)$$

$$C = (\rho_p^2 e^{2\sigma} + \rho_m^2 e^{-2\sigma})(\cos \alpha_p + \mathcal{K} \sin \alpha_p)^2 + (\rho_p^2 e^{-2\sigma} + \rho_m^2 e^{2\sigma})(\mathcal{K} \cos \alpha_p - \sin \alpha_p)^2 \quad (45)$$

where

$$\begin{aligned} \rho_m^p &= \frac{\rho_+ \pm \rho_-}{2}, \alpha_m^p = \frac{\alpha_+ \pm \alpha_-}{2} \\ \rho_\pm &= |r_{\text{fc}}(\pm\Omega, \Delta\omega_{\text{fc}})| \\ \alpha_\pm &= \arg(r_{\text{fc}}(\pm\Omega, \Delta\omega_{\text{fc}})) \end{aligned} \quad (46)$$

Ω is sideband frequency and was fixed to $\Delta\omega_{\text{fc},0}$ in Sec. II A-II D. \mathcal{K} is the optomechanical coupling factor of the interferometer,

$$\mathcal{K} = \left(\frac{\Omega_{\text{SQL}}}{\Omega} \right)^2 \frac{\gamma_{\text{ifo}}^2}{\Omega^2 + \gamma_{\text{ifo}}^2} \quad (47)$$

where Ω_{SQL} is frequency at which quantum noise reaches the standard quantum limit and γ_{ifo} is the interferometer bandwidth. In the case of KAGRA, $\Omega_{\text{SQL}} = 2\pi \times 76.4$ Hz, $\gamma_{\text{ifo}} = 2\pi \times 382$ Hz [15]. When $\phi = 0$, $\hat{N}_1(\phi = 0) = A$ and this represents the quantum noise of an optimally matched filter cavity with no injection and readout losses, (44) in [13].

From (40), frequency-independent phase noise of \hat{N}_1 can be calculated as

$$\hat{N}_{1,\text{avg}}(\phi) = \frac{\hat{N}_1(\delta\phi) + \hat{N}_1(-\delta\phi)}{2} = A \cos^2 \delta\phi + C \sin^2 \delta\phi \quad (48)$$

Frequency-dependent phase noise can be calculated by averaging $\hat{N}_1(\Delta\omega_{\text{fc},0} + \delta\Delta\omega_{\text{fc}})$ and $\hat{N}_1(\Delta\omega_{\text{fc},0} - \delta\Delta\omega_{\text{fc}})$. However, when there is detuning noise, there is also feedback from coherent control loop (39). As shown in FIG. 4, this feedback from coherent control loop is sent to the squeezer laser and changes the injection squeezing angle ϕ . Therefore, the frequency-dependent phase noise of \hat{N}_1 with feedback from coherent control loop can be calculated as

$$\begin{aligned} &\hat{N}_{1,\text{avg}}(\phi, \Delta\omega_{\text{fc},0}) \\ &= \frac{1}{2} \left\{ \hat{N}_1(-\delta\alpha_p(\Delta\omega_{\text{fc},0} + \delta\Delta\omega_{\text{fc}}, a, \rho), \Delta\omega_{\text{fc},0} + \delta\Delta\omega_{\text{fc}}) \right. \\ &\quad \left. + \hat{N}_1(-\delta\alpha_p(\Delta\omega_{\text{fc},0} - \delta\Delta\omega_{\text{fc}}, a, \rho), \Delta\omega_{\text{fc},0} - \delta\Delta\omega_{\text{fc}}) \right\} \quad (49) \end{aligned}$$

Note that frequency-dependent phase noise $\delta\alpha_p$ is small above cavity pole of the filter cavity ~ 60 Hz and we assumed that the gain of the coherent control loop below 60 Hz is large so that the feedback of the coherent control loop is perfect.

FIG. 6 and 7 shows quantum noise relative to coherent vacuum with filter cavity length noise $\delta L_{\text{fc}} = 0.3$ pm and 3 pm. The frequency-dependent phase noise with this scheme and with conventional scheme is shown as purple line and dotted purple line which are almost overlapping in FIG. 6. Parameters used in this calculation are shown in TABLE I. Unbalance of filter cavity reflectivity of CCSB is $\rho = 1.1$ and we assumed unbalance of amplitude of CCSB is $a = 1$ ($g \gg 1$). As shown in FIG. 6, frequency-dependent phase noise with this scheme and

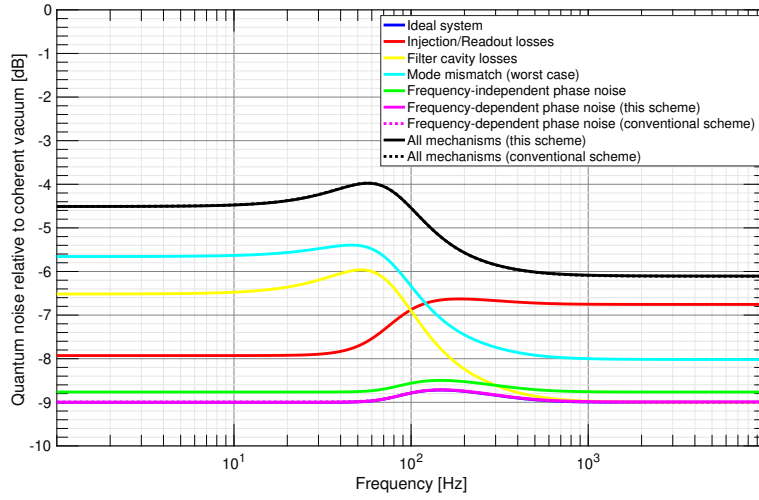


FIG. 6. Quantum noise relative to coherent vacuum with $\delta L_{fc} = 0.3$ pm. Solid purple and black lines are frequency-dependent phase noise and total noise with this scheme. Dotted purple and black lines are frequency-dependent phase noise and total noise with conventional scheme. The solid lines and dotted lines are overlapping since the effect of frequency-dependent phase noise is small.

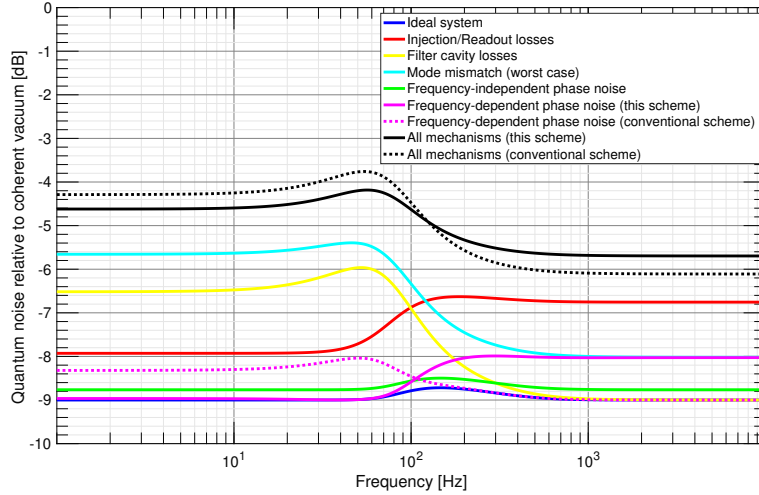


FIG. 7. Quantum noise relative to coherent vacuum with $\delta L_{fc} = 3$ pm.

conventional scheme is small and almost the same with $\delta L_{fc} = 0.3$ pm. However, as shown in FIG. 7, frequency-dependent phase noise with this scheme is suppressed at low frequency by the feedback from coherent control loop while it is increased at high frequency.

III. NOISE CALCULATION

The requirement of locking accuracy of the filter cavity (filter cavity length noise) δL_{fc} is 0.3 pm. In this section, we show that shot noise and PLL noise satisfy this requirement.

A. Shot noise

For simplicity, we assume that power of CCSB at OMC reflection are same, $P_+ = P_- = 10$ uW.

1. Shot noise of coherent control sidebands

Shot noise of CCSB is given by

$$P_{\text{shot}} = \sqrt{2\hbar\omega_0(P_+ + P_-)} \quad (50)$$

Here we assumed that carrier and CCSB frequencies are almost the same. This shot noise within filter cavity control bandwidth becomes filter cavity length noise by filter

cavity control loop. This shot noise is the most fundamental limit of the filter cavity error signal SNR. Starting from (11) and (14), we can write the shot noise contribution to the filter cavity length noise as follows,

$$\sqrt{P_+P_-}\frac{8\mathcal{F}}{\lambda}\delta L_{fc} > \sqrt{2\hbar\omega_0(P_+ + P_-)\Delta f} \quad (51)$$

$$\begin{aligned} \delta L_{fc} &> \frac{\lambda}{4\mathcal{F}}\sqrt{\frac{\hbar\omega_0}{2}\left(\frac{1}{P_+} + \frac{1}{P_-}\right)\Delta f} \\ &= 2.2 \times 10^{-17} \text{ m} \\ &\times \left(\frac{4360}{\mathcal{F}}\right)\left(\frac{10 \text{ uW}}{P_{\pm}}\right)^{1/2}\left(\frac{\Delta f}{10 \text{ Hz}}\right)^{1/2} \end{aligned} \quad (52)$$

where Δf is filter cavity control bandwidth and set by requirement of backscattering noise [19]. Using the parameters in TABLE I, the requirement of the filter cavity length noise $\delta L_{fc} = 0.3 \text{ pm}$ is not limited by the shot noise of CCSB.

2. Shot noise of junk light

When the filter cavity error signal is obtained at OMC reflection, junk light at OMC reflection contributes to the shot noise. We can compute the maximum power of this junk light at OMC reflection which allows not to spoil the filter cavity error signal as follows,

$$\sqrt{P_+P_-}\frac{8\mathcal{F}}{\lambda}\delta L_{fc} > \sqrt{2\hbar\omega_0P_{\text{junk}}\Delta f} \quad (53)$$

$$\begin{aligned} P_{\text{junk}} &< 32\frac{P_+P_-}{\hbar\omega_0\Delta f}\frac{\delta L_{fc}^2}{\lambda^2}\mathcal{F}^2 \\ &= 2.6 \text{ kW} \\ &\times \left(\frac{P_{\pm}}{10 \text{ uW}}\right)^2\left(\frac{\mathcal{F}}{4360}\right)^2\left(\frac{\delta L_{fc}}{0.3 \text{ pm}}\right)^2\left(\frac{10 \text{ Hz}}{\Delta f}\right) \end{aligned} \quad (54)$$

According to (54), using parameters in TABLE I, $P_{\text{junk}} < 2.6 \text{ kW}$ in order not to spoil the filter cavity error signal and this requirement can be satisfied in KAGRA [20].

B. PLL noise

The PLL which controls the relative phase between the squeezer laser and the coherent control laser can cause detuning noise. The PLL frequency noise reflected by the filter cavity can be written as

$$S_{\text{PLL},fc}(f) = \frac{S_{\text{PLL}}(\phi)f}{\sqrt{1 + (f/f_{fc})^2}} \quad (55)$$

where filter cavity half bandwidth is $f_{fc} = 57.3 \text{ Hz}$ and PLL phase noise is $S_{\text{PLL}}(\phi) = 5 \text{ } \mu\text{rad}/\sqrt{\text{Hz}}$ within PLL

control bandwidth $\sim 40 \text{ kHz}$. The PLL phase noise has been chosen so to have rms of PLL phase noise $\delta\phi_{\text{PLL}} = 1 \text{ mrad}$. The rms of PLL frequency noise reflected by the filter cavity is

$$\begin{aligned} \delta f_{\text{PLL},fc} &= \sqrt{\int df S_{\text{PLL},fc}^2(f)} \\ &= S_{\text{PLL}}(\phi)\sqrt{\int df \frac{f^2}{1 + (f/f_{fc})^2}} \\ &= S_{\text{PLL}}(\phi)f_{fc}\sqrt{\left(f - f_{fc}\arctan\frac{f}{f_{fc}}\right)} \end{aligned} \quad (56)$$

Integrating (56) between 0 Hz - 40 kHz, the rms of PLL frequency noise reflected by the filter cavity is $\delta f_{\text{PLL},fc} = 50 \text{ mHz}$. This corresponds to rms of filter cavity length noise $\delta L_{\text{PLL},fc} = 0.05 \text{ pm}$ which satisfies the requirement.

IV. CONCLUSION

We suggest a new length and alignment control scheme of a filter cavity with coherent control sidebands which are already used to control squeezing angle. It assures accurate detuning and alignment of the filter cavity with respect to squeezed vacuum states. It is shown that coherent control loop reshapes frequency-dependent phase noise with this scheme. The frequency-dependent phase noise at low frequency is suppressed by feedback from the coherent control loop while it is increased at high frequency. We also showed shot noise and PLL noise with this scheme satisfies the requirement of locking accuracy of the filter cavity.

ACKNOWLEDGMENTS

This work was supported by JSPS Grant-in-Aid for Scientific Research (Grants No. 18H01224, No. 18H01235 and No. 18K18763) and JST CREST (Grant No. JPMJCR1873). We thank Kentaro Komori for fruitful discussions.

Appendix A: Matrix formalism of misalignment

Input beam which includes HG 10 mode can be written as

$$E_{\text{in}} = \begin{pmatrix} U_{00} & U_{10} \end{pmatrix} \begin{pmatrix} a_0 \\ a_1 \end{pmatrix} E_0 e^{i\omega t} \quad (A1)$$

where a_0, a_1 is amplitude of HG 00, 10 mode. Filter cavity mode which is displaced in x axis by δx and tilted

around y axis by $\delta\theta$ with respect to input beam can be written as [16]

$$E_{fc} = \begin{pmatrix} U_{00} & U_{10} \end{pmatrix} M(\gamma) \begin{pmatrix} a_0 \\ a_1 \end{pmatrix} E_0 e^{i\omega t} \quad (\text{A2})$$

$$M(\gamma) = \begin{pmatrix} 1 & \gamma \\ -\gamma^* & 1 \end{pmatrix} \quad (\text{A3})$$

where γ is (15) and first order of γ is considered.

Reflection matrix of an optimally aligned filter cavity is

$$R_{fc}^{\text{align}} = \begin{pmatrix} r_{c0} & 0 \\ 0 & r_{c1} \end{pmatrix} \quad (\text{A4})$$

Reflection matrix of a misaligned filter cavity in the first order of γ, γ_r can be written as

$$\begin{aligned} R_{fc}^{\text{mis}}(\gamma, \gamma_r) &= M^*(\gamma_r) R_{fc}^{\text{align}} M(\gamma) \\ &= \begin{pmatrix} r_{c0} & r_{c0}\gamma + r_{c1}\gamma_r^* \\ -(r_{c0}\gamma_r + r_{c1}\gamma^*) & r_{c1} \end{pmatrix} \end{aligned} \quad (\text{A5})$$

Assuming that $a_0 = 1, a_1 = 0$ for input beam, reflection beam from the misaligned filter cavity can be written as

$$E_{\text{ref}} = [U_{00}r_{c0} - U_{10}(r_{c0}\gamma_r + r_{c1}\gamma^*)] E_0 e^{i\omega t} \quad (\text{A6})$$

Appendix B: Calculation of quantum noise

Calculation of quantum noise in this appendix is based on [13]. Quantum noise can be divided into three parts, noise due to vacuum fluctuations passing through the squeezer N_1 , noise due to vacuum fluctuations which do not pass through squeezer N_2 , noise due to vacuum fluctuations in the readout N_3 .

Quantum noise at the interferometer readout is given by

$$\begin{aligned} N(\zeta) &= |\bar{\mathbf{b}}_\zeta \cdot \mathbf{T}_1 \cdot v_1|^2 + |\bar{\mathbf{b}}_\zeta \cdot \mathbf{T}_2 \cdot v_2|^2 + |\bar{\mathbf{b}}_\zeta \cdot \mathbf{T}_3 \cdot v_3|^2 \\ &\equiv N_1 + N_2 + N_3 \end{aligned} \quad (\text{B1})$$

where $v_i = \sqrt{2\hbar\omega_0}\mathbf{I}$ ($i = 1, 2, 3$) is vacuum fluctuation and \mathbf{I} is 2×2 identity matrix. $\bar{\mathbf{b}}_\zeta = A_{\text{LO}}(\sin\zeta \cos\zeta)$ is local oscillator and $N(\zeta = 0)$ is the quantum noise in the quadrature containing the interferometer signal.

\mathbf{T}_1 is written as

$$\mathbf{T}_1 = \tau_{\text{ro}} \mathbf{T}_{\text{ifo}} (\mathbf{T}_{00} \mathbf{T}_{\text{fc}} + \mathbf{T}_{\text{mm}}) \mathbf{T}_{\text{inj}} \quad (\text{B2})$$

$$\mathbf{T}_{\text{ifo}} = \begin{pmatrix} 1 & 0 \\ -\mathcal{K} & 1 \end{pmatrix} \quad (\text{B3})$$

$$\mathbf{T}_{\text{fc}} = e^{i\alpha_m} \mathbf{R}_{\alpha_p} (\rho_p \mathbf{I} - i\rho_m \mathbf{R}_{\pi/2}) \quad (\text{B4})$$

$$\mathbf{T}_{00} = |t_{00}| \mathbf{R}_{\text{arg}(t_{00})}, \mathbf{T}_{\text{mm}} = |t_{\text{mm}}| \mathbf{R}_{\text{arg}(t_{\text{mm}})} \quad (\text{B5})$$

$$\mathbf{T}_{\text{inj}} = \tau_{\text{inj}} \mathbf{R}_\phi \begin{pmatrix} e^\sigma & 0 \\ 0 & e^{-\sigma} \end{pmatrix} \mathbf{R}_{-\phi} \quad (\text{B6})$$

where \mathbf{T}_{ifo} , \mathbf{T}_{fc} , \mathbf{T}_{inj} are transfer matrices of interferometer, optimally matched filter cavity and injection field, respectively. \mathbf{T}_{00} , \mathbf{T}_{mm} are mode matching and mode mismatch matrix.

τ_{inj} , τ_{ro} is injection, readout transmissivity and can be written as

$$\tau_{\text{inj}} = \sqrt{1 - \Lambda_{\text{inj}}^2} \quad (\text{B7})$$

$$\tau_{\text{ro}} = \sqrt{1 - \Lambda_{\text{ro}}^2} \quad (\text{B8})$$

where Λ_{inj}^2 , Λ_{ro}^2 are injection, readout losses.

t_{00} , t_{mm} can be written as $t_{00} = a_0 b_0^*$, $t_{\text{mm}} = \sum_{n=1}^{\infty} a_n b_n^*$ where a_n, b_n are complex coefficients when we express the squeezed vacuum states and the local oscillator in the basis of the filter cavity mode and can be written as

$$U_{\text{sqz}} = \sum_{n=0}^{\infty} a_n U_n, \text{ with } \sum_{n=0}^{\infty} |a_n|^2 = 1 \quad (\text{B9})$$

$$U_{\text{lo}} = \sum_{n=0}^{\infty} b_n U_n, \text{ with } \sum_{n=0}^{\infty} |b_n|^2 = 1 \quad (\text{B10})$$

where U_n are the orthogonal basis of spatial modes and U_0 is the filter cavity fundamental mode.

\mathbf{T}_2 is written as

$$\mathbf{T}_2 = \tau_{\text{ro}} \mathbf{T}_{\text{ifo}} \Lambda_2 \quad (\text{B11})$$

$$\Lambda_2 = \sqrt{1 - (|\tau_2(\Omega)|^2 + |\tau_2(-\Omega)|^2)/2} \quad (\text{B12})$$

$$\tau_2(\Omega) = (t_{00} r_{\text{fc}}(\Omega) + t_{\text{mm}}) \tau_{\text{inj}} \quad (\text{B13})$$

\mathbf{T}_3 is written as

$$\mathbf{T}_3 = \Lambda_{\text{ro}} \quad (\text{B14})$$

Quantum noise normalized with respect to shot noise level used in Sec. II E is

$$\hat{N} = \frac{N}{2\hbar\omega_0 A_{\text{LO}}^2} \quad (\text{B15})$$

For calculation of frequency-dependent phase noise, we can consider only N_1 since N_2 and N_3 are independent of \mathbf{T}_{fc} . From (B1)-(B8) and (B15), (42) can be derived.

- [2] B. P. Abbott *et al.* (LIGO Scientific Collaboration and Virgo Collaboration), Phys. Rev. X **9**, 031040 (2019).
- [3] C. M. Caves, Phys. Rev. D **23**, 1693 (1981).
- [4] J. Abadie *et al.* (LIGO Scientific Collaboration), Nat. Phys. **7**, 962 (2011).
- [5] M. Tse *et al.*, Phys. Rev. Lett. **123**, 231107 (2019).
- [6] F. Acernese *et al.* (Virgo Collaboration), Phys. Rev. Lett. **123**, 231108 (2019).
- [7] H. J. Kimble, Y. Levin, A. B. Matsko, K. S. Thorne, and S. P. Vyatchanin, Phys. Rev. D **65**, 022002 (2001).
- [8] B. P. Abbott *et al.* (LIGO Scientific Collaboration, Virgo Collaboration and KAGRA Collaboration), arXiv: 1304.0670 [gr-qc] .
- [9] Y. Zhao *et al.*, Phys. Rev. Lett. **124**, 171101 (2020).
- [10] H. A. Macleod, *Thin-Film Optical Filters*, 5th ed. (CRC Press, 2018).
- [11] L. McCuller *et al.*, Phys. Rev. Lett. **124**, 171102 (2020).
- [12] S. Chelkowski, H. Vahlbruch, K. Danzmann, and R. Schnabel, Phys. Rev. A **75**, 043814 (2007).
- [13] P. Kwee, J. Miller, T. Isogai, L. Barsotti, and M. Evans, Phys. Rev. D **90**, 062006 (2014).
- [14] H. Vahlbruch, M. Mehmet, K. Danzmann, and R. Schnabel, Phys. Rev. Lett. **117**, 110801 (2016).
- [15] E. Capocasa, M. Barsuglia, J. Degallaix, L. Pinard, N. Straniero, R. Schnabel, K. Somiya, Y. Aso, D. Tatsumi, and R. Flaminio, Phys. Rev. D **93**, 082004 (2016).
- [16] E. Morrison, B. J. Meers, D. I. Robertson, and H. Ward, Appl. Opt. **33**, 5041 (1994).
- [17] H. Kogelnik and T. Li, Appl. Opt. **5**, 1550 (1966).
- [18] K. L. Dooley, E. Schreiber, H. Vahlbruch, C. Affeldt, J. R. Leong, H. Wittel, and H. Grote, Opt. Express **23**, 8235 (2015).
- [19] L. McCuller and L. Barsotti, LIGO-T1800447 (2020).
- [20] K. Somiya, E. Hirose, and Y. Michimura, Phys. Rev. D **100**, 082005 (2019).